

Interplay of Electroweak Precision Observables and B Physics Observables

S. Heinemeyer

Instituto de Fisica de Cantabria (CSIC-UC), Santander, Spain

Indirect information about the possible scale of supersymmetry (SUSY) breaking is provided by B -physics observables (BPO) as well as electroweak precision observables (EWPO). We review the combination of the constraints imposed by recent measurements of the BPO $\text{BR}(b \rightarrow s\gamma)$, $\text{BR}(B_s \rightarrow \mu^+\mu^-)$, $\text{BR}(B_u \rightarrow \tau\nu_\tau)$ and ΔM_{B_s} with those obtained from the experimental measurements of the EWPO M_W , $\sin^2\theta_{\text{eff}}$, Γ_Z , $(g-2)_\mu$ and M_h . We perform a χ^2 fit to the parameters of the constrained minimal supersymmetric extension of the Standard Model (CMSSM), in which the SUSY-breaking parameters are universal at the GUT scale. Assuming that the lightest supersymmetric particle (LSP) provides the cold dark matter density preferred by WMAP and other cosmological data, we confirm the preference found previously for a relatively low SUSY-breaking scale, though there is some slight tension between the EWPO and the BPO.

1 Introduction

In order to achieve a simplification of the plethora of soft SUSY-breaking parameters appearing in the general MSSM, one assumption that is frequently employed is that (at least some of) the soft SUSY-breaking parameters are universal at some high input scale, before renormalization. One model based on this simplification is the constrained MSSM (CMSSM), in which all the soft SUSY-breaking scalar masses m_0 are assumed to be universal at the GUT scale, as are the soft SUSY-breaking gaugino masses $m_{1/2}$ and trilinear couplings A_0 . Further parameters are $\tan\beta$, the ratio of the two vacuum expectation values, and the sign of the Higgs mixing parameter μ .

Within the CMSSM we perform a combined χ^2 analysis [2] of electroweak precision observables (EWPO) [3], going beyond previous such analyses [4, 5] (see also Ref. [6]), and of B -physics observables (BPO), including some that have not been included before in comprehensive analyses of the SUSY parameter space (see, however, Ref. [7]). The set of EWPO included in the analysis is the W boson mass M_W , the effective leptonic weak mixing angle $\sin^2\theta_{\text{eff}}$, the total Z boson width Γ_Z , the anomalous magnetic moment of the muon $(g-2)_\mu$, and the mass of the lightest MSSM Higgs boson mass M_h . In addition, we include four BPO: the branching ratios $\text{BR}(b \rightarrow s\gamma)$, $\text{BR}(B_s \rightarrow \mu^+\mu^-)$ and $\text{BR}(B_u \rightarrow \tau\nu_\tau)$, and the B_s mass mixing parameter ΔM_{B_s} . For the evaluation of the BPO we assume minimal flavor violation (MFV) at the electroweak scale.

2 The χ^2 evaluation

Assuming that the nine observables listed above are uncorrelated, a χ^2 fit has been performed with

$$\chi^2 \equiv \sum_{n=1}^7 \left[\left(\frac{R_n^{\text{exp}} - R_n^{\text{theo}}}{\sigma_n} \right)^2 + 2 \log \left(\frac{\sigma_n}{\sigma_n^{\text{min}}} \right) \right] + \chi_{M_h}^2 + \chi_{B_s}^2. \quad (1)$$

Here R_n^{exp} denotes the experimental central value of the n th observable (M_W , $\sin^2 \theta_{\text{eff}}$, Γ_Z , $(g-2)_\mu$ and $\text{BR}(b \rightarrow s\gamma)$, $\text{BR}(B_u \rightarrow \tau\nu_\tau)$, ΔM_{B_s}), R_n^{theo} is the corresponding MSSM prediction and σ_n denotes the combined error (intrinsic, parametric (from m_t , m_b , α_s , $\Delta\alpha_{\text{had}}$), and experimental). Additionally, σ_n^{min} is the minimum combined error over the parameter space of each data set as explained below, and $\chi_{M_h}^2$ and $\chi_{B_s}^2$ denote the χ^2 contribution coming from the experimental limits on the lightest MSSM Higgs boson mass and on $\text{BR}(B_s \rightarrow \mu^+\mu^-)$, respectively, see Ref. [2] for details.

In order to take the m_t and m_b parametric uncertainties correctly into account, we evaluate the SUSY spectrum and the observables for each data point first for the nominal values $m_t = 171.4$ GeV [8]^a and $m_b(m_b) = 4.25$ GeV, then for $m_t = (171.4 + 1.0)$ GeV and $m_b(m_b) = 4.25$ GeV, and finally for $m_t = 171.4$ GeV and $m_b(m_b) = (4.25 + 0.1)$ GeV. The latter two evaluations are used by appropriate rescaling to estimate the full parametric uncertainties induced by the experimental uncertainties $\delta m_t^{\text{exp}} = 2.1$ GeV [8] and $\delta m_b(m_b)^{\text{exp}} = 0.11$ GeV. These parametric uncertainties are then added to the other errors (intrinsic, parametric (α_s , $\Delta\alpha_{\text{had}}$), and experimental).

In regions that depend sensitively on the input values of m_t and $m_b(m_b)$, such as the focus-point region [10] in the CMSSM, the corresponding parametric uncertainty can become very large. In essence, the ‘WMAP hypersurface’ moves significantly as m_t varies (and to a lesser extent also $m_b(m_b)$), but remains thin. Incorporating this large parametric uncertainty naively in eq. (1) would artificially suppress the overall χ^2 value for such points. This artificial suppression is avoided by adding the second term in eq. (1), where σ_n^{min} is the value of the combined error evaluated for parameter choices which minimize χ_n^2 over the full data set.

Throughout this analysis, we focus our attention on parameter points that yield the correct value of the cold dark matter density inferred from WMAP and other data, namely $0.094 < \Omega_{\text{CDM}} h^2 < 0.129$ [11]. The fact that the density is relatively well known restricts the SUSY parameter space to a thin, fuzzy ‘WMAP hypersurface’, effectively reducing its dimensionality by one. The variations in the EWPO and BPO across this hypersurface may in general be neglected, so that we may treat the cold dark matter constraint effectively as a δ function. We note, however, that for any given value of $m_{1/2}$ there may be more than one value of m_0 that yields a cold dark matter density within the allowed range, implying that there may be more than one WMAP line traversing the $(m_{1/2}, m_0)$ plane. Specifically, in the CMSSM there is, in general, one WMAP line in the coannihilation/rapid-annihilation funnel region and another in the focus-point region, at higher m_0 . Consequently, each EWPO and BPO may have more than one value for any given value of $m_{1/2}$. In the following, we restrict our study of the upper WMAP line to the part with $m_0 < 2000$ GeV for $\tan\beta = 10$ and $m_0 < 3000$ GeV for $\tan\beta = 50$, restricting in turn the range of $m_{1/2}$.

For our CMSSM analysis, the fact that the cold dark matter density is known from astrophysics and cosmology with an uncertainty smaller than 10 % fixes with proportional precision one combination of the SUSY parameters, enabling us to analyze the overall χ^2 value as a function of $m_{1/2}$ for fixed values of $\tan\beta$ and A_0 . The value of $|\mu|$ is fixed by the electroweak vacuum conditions (and $\mu > 0$ due to $(g-2)_\mu$), the value of m_0 is fixed with a small error by the dark matter density, and the Higgs mass parameters are fixed by the universality assumption. As in previous analyses, we consider various representative values

^aUsing the most recent experimental value, $m_t = 170.9 \pm 2.1$ GeV [9] would have a minor impact on our analysis.

of $A_0 \propto m_{1/2}$ for the specific choices $\tan\beta = 10, 50$.

3 The χ^2 analyses for EWPO, BPO and combined

Here we show the χ^2 results as a function of $m_{1/2}$, using eq. (1). As a first step, Fig. 1 displays the χ^2 distribution for the EWPO alone. In the case $\tan\beta = 10$ (left panel), we see a well-defined minimum of χ^2 for $m_{1/2} \sim 300$ GeV when $A_0 > 0$, which disappears for large negative A_0 and is not present in the focus-point region. The rise at small $m_{1/2}$ is due both to the lower limit on M_h coming from the direct search at LEP [12] and to $(g-2)_\mu$, whilst the rise at large $m_{1/2}$ is mainly due to $(g-2)_\mu$. The measurement of M_W leads to a slightly lower minimal value of χ^2 , but there are no substantial contributions from any of the other EWPO. The preference for $A_0 > 0$ in the coannihilation region is due to M_h , see the left plot in Fig. 4, and the relative disfavor for the focus-point regions is due to its mismatch with $(g-2)_\mu$. In the case $\tan\beta = 50$ (right panel), we again see a well-defined minimum of χ^2 , this time for $m_{1/2} \sim 400$ to 500 GeV, which is similar for all the studied values of A_0 . In this case, there is also a similar minimum of χ^2 for the focus-point region at $m_{1/2} \sim 200$ GeV. The increase in χ^2 at small $m_{1/2}$ is due to $(g-2)_\mu$ as well as M_h , whereas the increase at large $m_{1/2}$ is essentially due to $(g-2)_\mu$. Contrary to the $\tan\beta = 10$ case, M_h does not induce a large difference for the various A_0 values, see the right plot in Fig. 4. We note that the overall minimum of $\chi^2 \sim 2$ is similar for both values of $\tan\beta$, and represents an excellent fit in each case.

Fig. 2 shows the corresponding combined χ^2 for the BPO alone. For both values of $\tan\beta$, these prefer large values of $m_{1/2}$, reflecting the fact that there is no hint of any deviation from the SM, and the overall quality of the fit is good. Very small values of $m_{1/2}$ are disfavored, particularly in the coannihilation region with $A_0 > 0$, mainly due to $b \rightarrow s\gamma$. The focus-point region is generally in very good agreement with the BPO data, except at very low $m_{1/2} \lesssim 400$ GeV for $\tan\beta = 50$.

Finally, we show in Fig. 3 the combined χ^2 values for the EWPO and BPO, computed in accordance with eq. (1). We see that the global minimum of $\chi^2 \sim 4.5$ for both values of $\tan\beta$. This is quite a good fit for the number of experimental observables being fitted, and the $\chi^2/\text{d.o.f.}$ is similar to the one for the EWPO alone. This increase in the total χ^2 reflects the fact that the BPO exhibit no tendency to reinforce the preference of the EWPO for small $m_{1/2}$. However, due to the relatively large experimental and theoretical errors for the BPO, no firm conclusion in any direction can be drawn yet. The focus-point region is disfavored for both values of $\tan\beta$ by comparison with the coannihilation region, though this effect is slightly less important for $\tan\beta = 50$. For $\tan\beta = 10$, $m_{1/2} \sim 300$ GeV and $A_0 > 0$ are preferred, whereas, for $\tan\beta = 50$, $m_{1/2} \sim 600$ GeV and $A_0 < 0$ are preferred. This change-over is largely due to the impact of the LEP M_h constraint for $\tan\beta = 10$ (see the left plot of Fig. 4) and the $b \rightarrow s\gamma$ constraint for $\tan\beta = 50$ (see Fig. 6 in Ref. [2]). Corresponding mass predictions for the SUSY particles can be found in Ref. [2].

4 Acknowledgments

We thank J. Ellis, K.A. Olive, A.M. Weber and G. Weiglein for collaboration on the work presented here. Work supported in part by the European Community's Marie-Curie Research Training Network under contract MRTN-CT-2006-035505 'Tools and Precision Calculations for Physics Discoveries at Colliders'

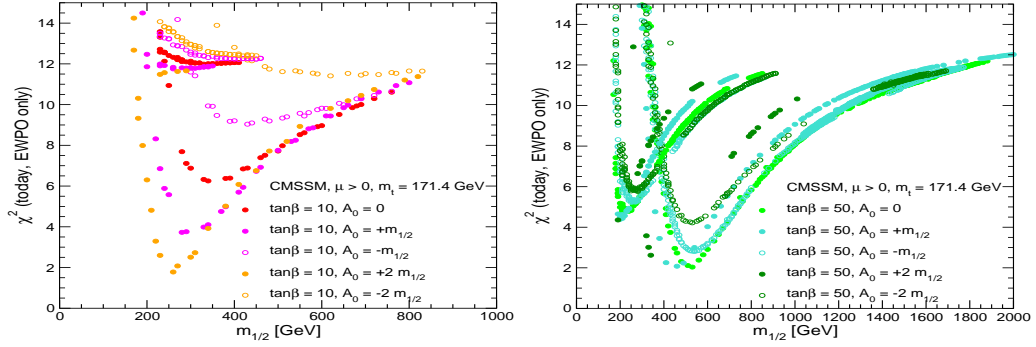


Figure 1: The combined χ^2 function for the electroweak observables M_W , $\sin^2 \theta_{\text{eff}}$, Γ_Z , $(g-2)_\mu$ and M_h , evaluated in the CMSSM for $\tan \beta = 10$ (left) and $\tan \beta = 50$ (right) for various discrete values of A_0 .

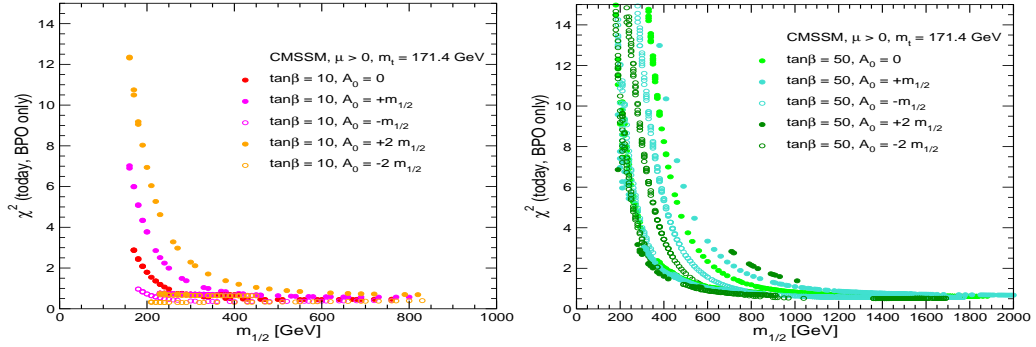


Figure 2: The combined χ^2 function for the B physics observables $\text{BR}(b \rightarrow s\gamma)$, $\text{BR}(B_s \rightarrow \mu^+\mu^-)$, $\text{BR}(B_u \rightarrow \tau\nu_\tau)$ and ΔM_{B_s} , evaluated in the CMSSM for $\tan \beta = 10$ (left) and $\tan \beta = 50$ (right) for various discrete values of A_0 .

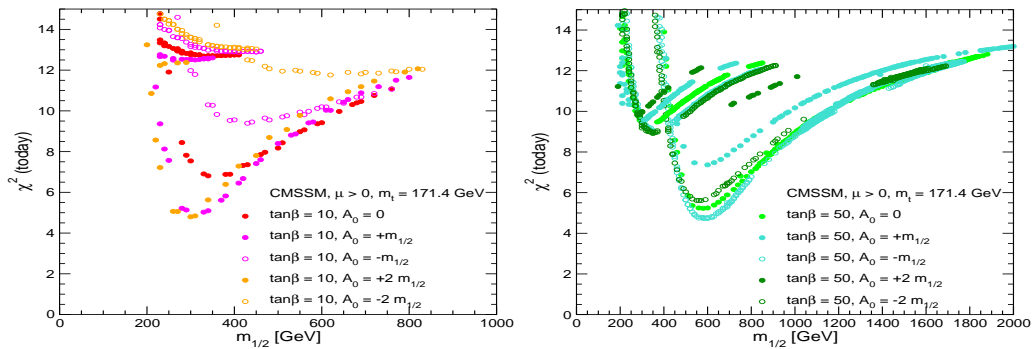


Figure 3: The combined χ^2 function for the EWPO and the BPO, evaluated in the CMSSM for $\tan \beta = 10$ (left) and $\tan \beta = 50$ (right) for various discrete values of A_0 .

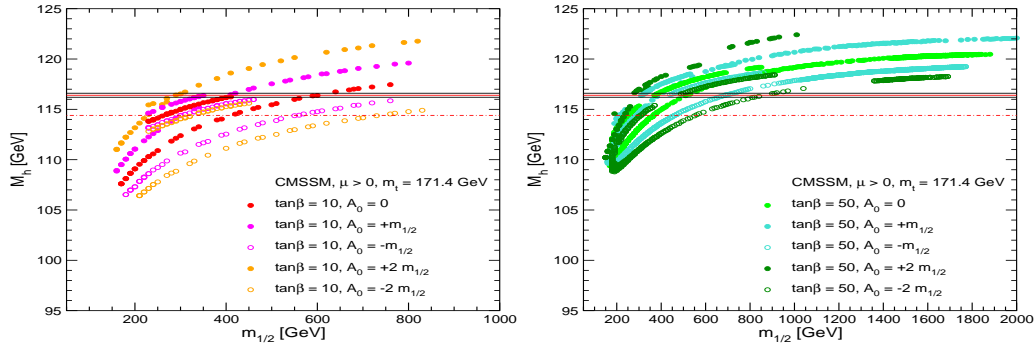


Figure 4: The CMSSM predictions for M_h as functions of $m_{1/2}$ with (a) $\tan\beta = 10$ and (b) $\tan\beta = 50$ for various A_0 . We also show the present 95% C.L. exclusion limit of 114.4 GeV and a hypothetical LHC measurement of $M_h = 116.4 \pm 0.2$ GeV. The results have been obtained with FeynHiggs [13].

References

- [1] Slides: ilcagenda.linearcollider.org/contributionDisplay.py?contribId=52&sessionId=69&confId=1296
- [2] J. Ellis, S. Heinemeyer, K. Olive, A.M. Weber and G. Weiglein, *JHEP* **0708** (2007) 083 [arXiv:0706.0652 [hep-ph]].
- [3] S. Heinemeyer, W. Hollik and G. Weiglein, *Phys. Rept.* **425** (2006) 265 [arXiv:hep-ph/0412214].
- [4] J. Ellis, S. Heinemeyer, K. Olive and G. Weiglein, *JHEP* **0502** (2005) 013 [arXiv:hep-ph/0411216].
- [5] J. Ellis, S. Heinemeyer, K. Olive and G. Weiglein, *JHEP* **0605** (2006) 005 [arXiv:hep-ph/0602220].
- [6] J. Ellis, K. Olive, Y. Santoso and V. Spanos, *Phys. Rev. D* **69** (2004) 095004 [arXiv:hep-ph/0310356]; B. Allanach and C. Lester, *Phys. Rev. D* **73** (2006) 015013 [arXiv:hep-ph/0507283]; B. Allanach, *Phys. Lett. B* **635** (2006) 123 [arXiv:hep-ph/0601089]; R. de Austri, R. Trotta and L. Roszkowski, *JHEP* **0605** (2006) 002 [arXiv:hep-ph/0602028]; *JHEP* **0704** (2007) 084 [arXiv:hep-ph/0611173]; arXiv:0705.2012 [hep-ph]; B. Allanach, C. Lester and A. M. Weber, *JHEP* **0612** (2006) 065 [arXiv:hep-ph/0609295]; B. Allanach, K. Cranmer, C. Lester and A. M. Weber, arXiv:0705.0487 [hep-ph]; O. Buchmueller et al., arXiv:0707.3447 [hep-ph].
- [7] G. Isidori, F. Mescia, P. Paradisi and D. Temes, *Phys. Rev. D* **75** (2007) 115019 [arXiv:hep-ph/0703035]; M. Carena, A. Menon and C. Wagner, *Phys. Rev. D* **76** (2007) 035004 [arXiv:0704.1143 [hep-ph]].
- [8] E. Brubaker et al. [Tevatron Electroweak Working Group], arXiv:hep-ex/0608032, see: tevewwg.fnal.gov/top/.
- [9] Tevatron Electroweak Working Group, arXiv:hep-ex/0703034.
- [10] J. Feng, K. Matchev and T. Moroi, *Phys. Rev. Lett.* **84** (2000) 2322 [arXiv:hep-ph/9908309]; *Phys. Rev. D* **61** (2000) 075005 [arXiv:hep-ph/9909334]; J. Feng, K. Matchev and F. Wilczek, *Phys. Lett. B* **482** (2000) 388 [arXiv:hep-ph/0004043]; J. Feng and K. Matchev, *Phys. Rev. D* **63** (2001) 095003 [arXiv:hep-ph/0011356].
- [11] C. Bennett et al., *Astrophys. J. Suppl.* **148** (2003) 1 [arXiv:astro-ph/0302207]; D. Spergel et al. [WMAP Collaboration], *Astrophys. J. Suppl.* **148** (2003) 175 [arXiv:astro-ph/0302209]; D. Spergel et al. [WMAP Collaboration], arXiv:astro-ph/0603449.
- [12] LEP Higgs working group, *Phys. Lett. B* **565** (2003) 61 [arXiv:hep-ex/0306033]; *Eur. Phys. J. C* **47** (2006) 547 [arXiv:hep-ex/0602042].
- [13] S. Heinemeyer, W. Hollik and G. Weiglein, *Comp. Phys. Commun.* **124** 2000 76 [arXiv:hep-ph/9812320]; *Eur. Phys. J. C* **9** (1999) 343 [arXiv:hep-ph/9812472]; G. Degrandi, S. Heinemeyer, W. Hollik, P. Slavich and G. Weiglein, *Eur. Phys. J. C* **28** (2003) 133 [arXiv:hep-ph/0212020]; M. Frank, T. Hahn, S. Heinemeyer, W. Hollik, H. Rzehak and G. Weiglein, *JHEP* **0702** (2007) 047 [arXiv:hep-ph/0611326]; see: www.feynhiggs.de.